both metal centers. In the symmetry of the problem, C_i, there are two irreducible representations: a_u and a_g. The LUMO, along with all other orbitals showing copper(II) character, must belong to the irreducible representation a_g. The copper(I) orbitals may belong to either representation, and the symmetries of these energy levels are denoted in Figure 4. The transitions arising from the a_u copper(I) orbitals will be of the strongest intensity. The transitions originating on the a_g copper(II) orbitals will be much weaker, since they occur via a vibronic mechanism. The broad absorption at 18 200 cm^{-1} is tentatively assigned to the transitions arising from the $a_g + a_u$ copper(I) orbitals at the bottom of the energy level diagram. Below 12 500 cm^{-1} are the typical copper(II) d-d transitions, with the sharp maximum at about 11 000 cm^{-1} attributable to transitions arising from the copper(I) a_u orbitals lying among the copper(II) d orbitals. Unfortunately, the nature of the sample precludes further investigation of this hypothesis via polarized spectroscopy.

There has been some work performed on analogous systems which support the above assignments. In the salts $Cu^{II}(NH_3)_4(Cu^{I}Br_2)_2$ and $Cu^{II}(NH_3)_4(Cu^{I}Cl_2)_2 \cdot H_2O$, the copper halide chains, consisting of edge-sharing $CuCl_4^{3-}$ tetrahedra, are cocrystallized parallel to stacks of square-planar $Cu^{II}(NH_3)_4^{2+}$ ions.[13a] The square-planar copper(II) ions are isolated from the copper(I) halide chains, with no ligands in the axial positions for the bromide and water molecules in the axial positions (2.73 Å) in the chloride. In the iodide analogue, $Cu^{II}(NH_3)_4(Cu^{I}I_2)_2$, the square-planar Cu(II) ions serve to bridge the copper(I) iodide chains and thus have iodide ions in the axial positions.[13b] In other words, in the chloride and bromide salts the plane of the $Cu(NH_3)_4^{2+}$ ion is perpendicular to the copper(I) halide chain axis, but in the iodide salt this plane is tilted, allowing the bridging iodide ions in the copper(I) chain to occupy the axial positions in the $Cu^{II}(NH_3)_4^{2+}$ ion. The chloride and bromide salts are both violet, a fact explained by the d-d transitions in a square-planar field of ammonia ligands. The iodide, however, is deep green, a result which the authors attribute to an intervalence charge transfer. The bridging network in the iodide salt is somewhat similar to that of the title compound, with the latter having additional shorter bridges involving the equatorial chloride ions. The fact that a significant change in the color of the iodide is brought on by such a weak bridge further supports the above intervalence assignments.

(13) (a) Baglio, J. A.; Vaughan, P. A. *J. Inorg. Nucl. Chem.* **1970**, *32*, 803. (b) Baglio, J. A.; Weakhem, H. A.; Demlio, F.; Vaughan, P. A. *J. Inorg. Nucl. Chem.* **1970**, *32*, 795.

Conclusions

The crystal structure, absorption spectroscopy, and EHMO calculations all support a class II Robin and Day classification for the title compound. The crystal structure reveals a chloride bridge between the Cu(I) and Cu(II) centers in this salt, a result which points to an interaction between the metal centers. The EHMO calculations performed show a mechanism for the intervalence charge transfer to occur; a purely Cu(II) LUMO molecular orbital with several lower lying molecular orbitals showing strong Cu(I) character. The broad absorption band, centered in a region where no absorption exists for either the Cu(I) or Cu(II) chromophore taken separately, supports such a picture.

Acknowledgment. This research was supported by NSF Grant DMR-8803382 and PRF Grant 20215-AC3-C. The X-ray diffraction facility was established through funds provided by NSF Grant CHE-8408407 and The Boeing Co.

Supplementary Material Available: Tables of X-ray data collection parameters, atomic coordinates and isotropic thermal parameters for non-hydrogen atoms, anisotropic thermal parameters for non-hydrogen atoms, and hydrogen atom positions and isotropic thermal parameters (3 pages); a structure factor table (4 pages). Ordering information is given on any current masthead page.

Contribution from the Central Research and Development Department, E. I. du Pont de Nemours and Company, Wilmington, Delaware 19880-0328, and Steacie Institute for Molecular Sciences, National Research Council of Canada, Ottawa, Ontario, Canada K1A 0R9

EPR Spectra of $(C_5Me_5)MoCl_2(PMe_3)_2$ in Solution and in Single Crystals of $(C_5Me_5)MoCl(PMe_3)_2(N_2)$†

R. T. Baker,*,‡ J. R. Morton,*,§ K. F. Preston,*,§ A. J. Williams,§ and Y. Le Page§

Received August 3, 1989

EPR spectra of the d^3 species $Cp^*MoCl_2(PMe_3)_2$ ($Cp^* = C_5Me_5$) have been observed both in solution at 173 K and in orthorhombic single crystals of $Cp^*MoCl(PMe_3)_2(N_2)$ at 77K. $C_{16}H_{33}ClMoN_2P_2$ is orthorhombic, of space group $P2_12_12_1$, with $a = 14.7195$ (11) Å, $b = 16.4715$ (16) Å, $c = 8.9180$ (6) Å, $V = 2162.2$ (3) Å^3, $Z = 4$, $R = 0.052$, and $R_w = 0.060$ for 1833 reflections. The matrices of **g** and the ^{95}Mo hyperfine interaction indicate that the unpaired spin population resides primarily in the $4d_{z^2}$ orbital of the molybdenum atom. However, considerable anisotropy was also apparent in the ^{31}P hyperfine interactions, whence it is concluded that some unpaired spin is to be found in the phosphorus 3p orbitals. These conclusions confirm recent Fenske-Hall type molecular orbital descriptions of the model compound $CpMoCl_2(PH_3)_2$.

Introduction

In the course of our research into the synthesis of early-transition-metal complexes containing terminal PR_2^- ligands,[1] we attempted to prepare new, low-valent W and Mo starting materials such as the 16-electron compound "$Cp^*MoCl(PMe_3)_2$". Instead of the latter, we obtained[2] dark blue crystals of the 18-electron dinitrogen complex $Cp^*MoCl(PMe_3)_2(N_2)$ contaminated with the red-brown, 17-electron complex $Cp^*MoCl_2(PMe_3)_2$. Upon finding crystals of the two compounds to be isomorphous, we undertook a single-crystal EPR study of the paramagnetic dichloro compound doped into diamagnetic crystals of the dinitrogen complex.

A general EHMO bonding analysis of $CpML_4$ piano stool complexes has been reported previously,[3] and a recent Fenske-Hall calculation[4] by Poli et al. on $CpMoCl_2(PH_3)_2$ implicated Mo-P

† NRCC No. 31480; Du Pont No. 5177.
‡ Du Pont.
§ National Research Council of Canada.

(1) (a) Baker, R. T.; Whitney, J. F.; Wreford, S. S. *Organometallics* **1983**, *2*, 1049; *Inorg. Chem.*, submitted for publication. (b) Baker, R. T.; Calabrese, J. C.; Krusic, P. J.; Tulip, T. H.; Wreford, S. S. *J. Am. Chem. Soc.* **1983**, *105*, 6763.
(2) Baker, R. T.; Calabrese, J. C.; Harlow, R. L.; Williams, I. D. *Organometallics*, submitted for publication.
(3) Kubacek, P.; Hoffmann, R.; Havlas, Z. *Organometallics* **1982**, *1*, 180.
(4) Krueger, S. T.; Poli, R.; Rheingold, A. L.; Stanley, D. L. *Inorg. Chem.* **1989**, *28*, 4599.

0020-1669/91/1330-0113$02.50/0

π-bonding in the singly occupied molecular orbital. The experimental results described herein confirm contributions from Mo 4d and P 3p orbitals to the SOMO.

Experimental Section

All preparations were conducted in a Vacuum Atmospheres glovebox with continuous dry nitrogen flush. Solvents were purified by standard techniques and distilled from sodium- or potassium–benzophenone ketyl. The literature method[5] was used to prepare $(Cp^*MoCl_4)_2$. PMe_3 (Strem) was used as received.

1. Preparation of $Cp^*MoCl(PMe_3)_2(N_2)$. To a solution of 3.4 g (45 mmol) of PMe_3 in 200 mL of THF was added 7.46 g (10 mmol) of $(Cp^*MoCl_4)_2$ and 201.4 g of 0.7% Na/Hg amalgam (61 mmol). The solution turned red-brown and then blue-green. After being stirred vigorously for 20 h, the solution was filtered through Celite and evaporated in vacuo. The residue was extracted with 200 mL of hexane, the extract was concentrated to 50 mL in vacuo, and the resulting blue crystals were filtered off, washed with 2 × 10 mL of cold pentane, and dried in vacuo. The yield was 4.13 g. Additional crops brought the total yield of the title complex to 7.268 g (81%). The product was invariably contaminated with $Cp^*MoCl_2(PMe_3)_2$, which cocrystallizes with the title complex.

2. Preparation of $Cp^*MoCl_2(PMe_3)_2$. This complex was prepared as above by using only 4 equiv of Na/Hg amalgam per Mo dimer. Workup was identical, yielding red-brown crystals of $Cp^*MoCl_2(PMe_3)_2$ in 80% yield.

3. EPR Spectroscopy and X-ray Crystallography. EPR spectra were obtained with a Varian Associates E-12 spectrometer equipped to operate between 4 and 300 K. The microwave frequency and magnetic field strength were continuously monitored and recorded for each spectral line. The parameters of the spin Hamiltonian were calculated from these observations by computerized diagonalization of the spin matrix. The procedure used depended on whether a liquid-phase or a single-crystal spectrum was being analyzed.

Orthorhombic single crystals of $Cp^*MoCl(PMe_3)_2(N_2)$ containing about 2% of the dichloro analogue were grown in *n*-pentane by slow removal of the solvent at 220 K. Examination of the mother liquor in the EPR spectrometer at 173 K revealed a well-resolved liquid-phase spectrum. This spectrum, which at sufficiently high sensitivity revealed not only ^{31}P but also ^{95}Mo hyperfine structure, was analyzed by a statistical method described several years ago.[6] The spectrum of $Cp^*MoCl_2(PMe_3)_2$ was also examined in the solid phase, trapped in single crystals of $Cp^*MoCl(PMe_3)_2(N_2)$. Crystals of the latter are usually monoclinic, but in the presence of the dichloro compound, an orthorhombic (space group $P2_12_12_1$) phase can be isolated. The crystal structure of this orthorhombic phase was determined on a Nonius X-ray diffractometer. The cell parameters were obtained from the centerings of 27 reflections with 2θ values in the range 30–35°. Diffracted intensities were measured on a crystal 0.30 × 0.30 × 0.20 mm^3 by using Mo Kα radiation up to a 45° Bragg angle and an $\omega/2\theta$ scan with a 1:2 angular speed ratio. The 2480 measurements reduced to 2211 unique reflections with R_{sym} of 2.8%; 1833 of these had $I_{net} > 2.5\sigma(I_{net})$ and were considered to be observed. The structure was solved by direct methods, and all non-hydrogen atoms were refined anisotropically (200 parameters) with a final residual of 0.053, $R_w = 0.060$, and goodness of fit = 0.41. The maximum shift/σ ratio was 0.326, and maximum electron density residuals of 0.48 e/Å^3 were located near Mo.

For the EPR experiments, an orthorhombic crystal of $Cp^*MoCl(PMe_3)_2(N_2)$ containing about 2% of the paramagnetic dichloro impurity was oriented by XRD so that one of its three orthorhombic axes was parallel to the length of the tube, the direction of one of the other two axes being indicated by a fine needle attached to the tube. The oriented crystal was sealed into a 4-mm-o.d. Suprasil tube with epoxy cement. When the tube was placed in the cold-finger Dewar flask inside the microwave cavity of the spectrometer, this needle moved over a horizontal brass protractor graduated every 5° of arc. By rotation of the Suprasil tube about a vertical axis, the magnetic field of the spectrometer explored in increments of 5 or 10° one of the crystallographic planes of the sample. Three separate samples were necessary in order to explore all three planes of the orthorhombic unit cell. Individual spectra yielded values of the *g* factor and the ^{31}P,^{95}Mo hyperfine interactions.

Results

1. X-ray Diffraction. Doped crystals of $Cp^*MoCl(PMe_3)_2(N_2)$ crystallize in the space group $P2_12_12_1$, the unit cell having the following dimensions: $a = 14.7195$ (11) Å, $b = 16.4715$ (16) Å, $c = 8.9180$ (6) Å. The atomic coordinates were approximately related to those of the dichloro compound[2] by the transformation $x, y, -z$, indicating that the structure models were similar but had opposite hands. With nonchiral molecules such as these, the hand has to do with the stacking rather than the molecule, and other crystals of either hand could have been found. The N_2 ligand prefers the Cl1 site rather than a random distribution over Cl1 and Cl2 sites. The fractional coordinates of the non-hydrogen atoms are given in Table I. It should be remembered that they do not correspond to a pure, but to a doped compound. The architecture of the molecules is that of the dichloro compound, but the stacking shows some differences. For example, the Mo–C(0) vectors differ by about 10°.

Table I. Atomic Positions in the Orthorhombic Unit Cell of $Cp^*MoCl(N_2)(PMe_3)_2$ in the Crystallographic *abc* Axis System[a]

atom[b]	*x*	*y*	*z*	B_{iso}/Å^2
Mo	0.99178 (6)	0.63160 (6)	0.18218 (12)	3.26 (4)
P1	0.86892 (23)	0.55611 (23)	0.3105 (5)	4.25 (17)
P2	1.0787 (3)	0.55073 (24)	0.0008 (5)	4.36 (18)
Cl	0.8767 (3)	0.60878 (23)	−0.0240 (5)	5.58 (19)
N1	1.0630 (11)	0.5476 (12)	0.3261 (20)	5.3 (9)
N2	1.0895 (13)	0.5224 (12)	0.3797 (24)	5.5 (9)
C1	1.0689 (15)	0.7533 (11)	0.1058 (24)	6.1 (10)
C2	1.0910 (11)	0.7294 (10)	0.255 (3)	7.4 (14)
C3	1.0082 (14)	0.7344 (7)	0.3510 (14)	4.7 (7)
C4	0.9406 (10)	0.7600 (8)	0.2420 (19)	4.3 (7)
C5	0.9825 (14)	0.7694 (10)	0.1008 (17)	5.1 (8)
C6	1.1493 (21)	0.7628 (13)	0.012 (4)	16.8 (23)
C7	1.1855 (12)	0.7151 (12)	0.329 (4)	15.1 (21)
C8	1.003 (3)	0.7334 (9)	0.5040 (21)	12.7 (20)
C9	0.8443 (11)	0.7874 (9)	0.279 (3)	8.8 (14)
C10	0.9327 (19)	0.8027 (10)	−0.0258 (23)	10.5 (15)
C11	0.8537 (11)	0.4541 (9)	0.2439 (21)	6.7 (9)
C12	0.8797 (12)	0.5368 (13)	0.5035 (21)	7.7 (10)
C13	0.7508 (9)	0.5916 (9)	0.3020 (21)	6.0 (8)
C21	1.0847 (13)	0.5824 (10)	−0.2008 (19)	7.4 (10)
C22	1.1961 (12)	0.5265 (11)	0.0436 (23)	7.5 (10)
C23	1.0349 (13)	0.4486 (10)	−0.0221 (23)	7.8 (10)

[a] Estimated standard deviations in parentheses refer to last digit printed. [b] Atom labeling as in Figure 3.

Table II. Line Positions, M_I Values, and Microwave Frequencies for the EPR Spectrum of $Cp^*MoCl_2(PMe_3)_2$ in *n*-Pentane at 173 K

field/G	M_I^{95}	M_I^{31}	freq/MHz
3146.16	−2.5	1.0	9026.18
3161.14	−2.5	0.0	9026.18
3176.67	−2.5	−1.0	9026.18
3180.26	−1.5	1.0	9026.18
3196.36	−1.5	0.0	9026.18
3282.58	0.5	−1.0	9026.41
3303.65	1.5	0.0	9026.41
3318.77	1.5	−1.0	9026.41
3340.49	2.5	0.0	9026.41
3356.13	2.5	−1.0	9026.41

2. EPR Spectroscopy. At low spectrometer sensitivity, the liquid-phase spectrum consisted of three lines of relative intensity 1:2:1, the latter hyperfine structure being due to the presence of two ^{31}P nuclei ($I_P = {}^1/_2$) in the paramagnetic compound. At higher sensitivity several satellites of the main spectrum were apparent on either side of the central features. These satellites were due to a finite (ca. 25%) concentration of magnetic isotopes of molybdenum, of which ^{95}Mo($I_{Mo} = {}^5/_2$) is the most abundant. A total of 10 lines in the satellite manifold could be accurately measured without interference from the central features. The results of these measurements, given in Table II, on the basis of the statistical method referred to above, yielded the following constants for the isotropic spin Hamiltonian:

$$g = 1.983\,57 \pm 0.000\,07 \qquad a_{95} = -99.4 \pm 0.2 \text{ MHz}$$

$$a_{31} = +42.7 \pm 0.5 \text{ MHz}$$

The relative signs of the two hyperfine constants could not be determined experimentally but were assumed from the known

(5) Murray, R. C.; Blum, L.; Liu, A.; Schrock, R. R. *Organometallics* **1985**, *4*, 953.
(6) Morton, J. R.; Preston, K. F. *J. Chem. Phys.* **1980**, *73*, 4914.

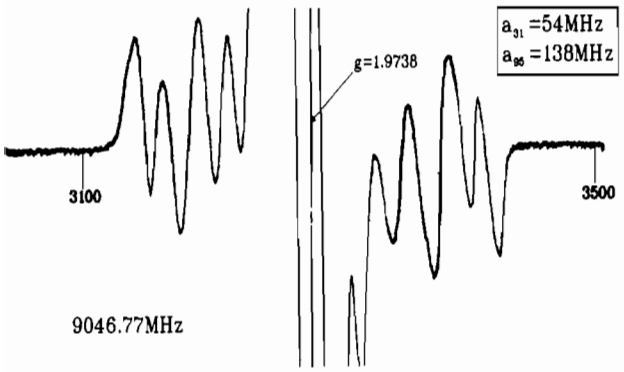

Figure 1. EPR spectrum of $Cp^*MoCl_2(PMe_3)_2$ in a single crystal of orthorhombic $Cp^*MoCl(N_2)(PMe_3)_2$ at 77 K, with B_0 parallel to the *c* axis.

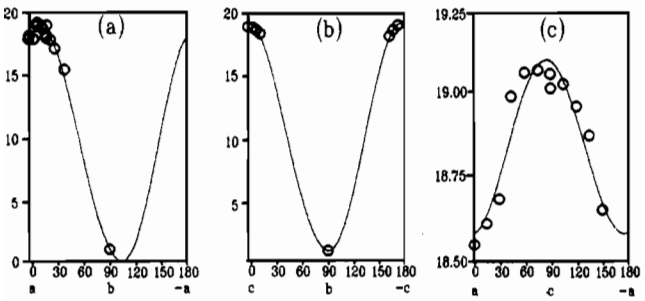

Figure 2. Graphs of the ^{95}Mo hyperfine interaction $10^{-3}a_{95}^2/MHz^2$ of $Cp^*MoCl_2(PMe_3)_2$ in an orthorhombic single crystal of $Cp^*Cl(N_2)(PMe_3)_2$ for (a) the *ab* plane, (b) the *bc* plane, and (c) the *ac* plane. The sinusoidal curves are least-squares fitted to the experimental points.

negative magnetic moment of ^{95}Mo and positive magnetic moment of ^{31}P. The errors quoted above are one standard deviation.

The single-crystal data were handled as follows: the matrices of $\mathbf{g}^2$ and $\mathbf{a}_{95}^2/MHz^2$ were assembled in the orthorhombic axis system by plotting these parameters as a function of angle as B_0 explored the three crystallographic planes.[7] The ^{95}Mo hyperfine structure of the single-crystal spectra was readily visible when B_0 lay anywhere in the *ac* plane (Figure 1) but became immeasurably small as B_0 approached the *b* axis. The value of the ^{95}Mo hyperfine interaction for B_0 parallel to *b* could not, therefore, be measured by placing B_0 along *b*. Instead, it was estimated from graphs of a_{95}^2 versus angle in the *ab* and *bc* planes. A knowledge of the isotropic value of $\mathbf{a}_{95}$ was also useful in making this estimate. A nonzero off-diagonal element in the tensor $\mathbf{a}_{95}^2/MHz^2$ was apparent only for the *ab* plane (Figure 2a), and at angles between B_0 and the *a* axis greater than 40°, the ^{95}Mo hyperfine structure disappeared under the central features. The best estimate of a_{95}^2 for B_0 parallel to the *b* axis was 1000 ± 500 MHz^2, obtained from the trace of the tensor of $\mathbf{a}_{95}^2$ and the above isotropic value of $\mathbf{a}_{95}$. In Figure 2a experimental points obtained every 5° near the *a* axis clearly indicate a small *ab* off-diagonal element, whereas in Figure 2b,c it is equally clear that the *bc* and *ac* off-diagonal elements are zero. The lines in Figure 2 are the results of a computerized least-squares fit of sinusoidal curves to the data points. It must be pointed out, however, that in Figure 2a,b the curves are forced through the 1000-MHz^2 point obtained as described above for B_0 parallel to the *b* axis.

The matrix $\mathbf{g}^2$ was obtained from the central features of the spectrum (even isotopes of Mo). The spectral lines were rather broad, however, due to the incomplete resolution of hyperfine interactions with the two ^{31}P nuclei. Their hyperfine interactions were not always equal, and the central feature was sometimes a doublet (Figure 1), sometimes a triplet, but most often a broad line of indeterminate structure. The ^{31}P structure was often slightly better resolved in the ^{95}Mo manifold than in the central features. It was not possible, however, to assemble the tensor of $\mathbf{a}_{31}^2/MHz^2$

(7) Morton, J. R.; Preston, K. F. *J. Magn. Reson.* **1983**, *52*, 457.

Table III. Matrices of $\mathbf{g}^2$ and $\mathbf{a}_{95}^2/MHz^2$ for $Cp^*MoCl_2(PMe_3)_2$ in Single Crystals of $Cp^*MoCl(N_2)(PMe_3)_2$ and Principal Values of $\mathbf{g}^2$, $\mathbf{g}$, $\mathbf{a}_{95}^2/MHz^2$, and $\mathbf{a}_{95}/MHz$, Together with Their Principal Direction Cosines in the *abc* Axis System

tensor in *abc* axes				principal values and their direction cosines		
			$\mathbf{g}^2$	4.0053	3.8937	3.8957
			$\mathbf{g}$	2.0013	1.9732	1.9738
3.8991	−0.0239	0.000		−0.2196	0.9756	0.0000
−0.0239	3.9999	0.0000		0.9756	0.2196	0.0000
0.0000	0.0000	3.8957		0.0000	0.0000	1.0000
			$\mathbf{a}_{95}^2$	101.1	18799	19000
			$\mathbf{a}_{95}$	10.1	137.1	137.8
17900	4000	0		−0.2193	0.9757	0.0000
4000	1000	0		0.9757	0.2193	0.0000
0	0	19000		0.0000	0.0000	1.0000

although the spectrum of Figure 1 is evidence of considerable anisotropy. One ^{31}P nucleus has a hyperfine interaction of ca. 50 MHz, while that of the other is lost in the line width and could be 15 MHz or even less. It is worth noting that the direction of maximum hyperfine interaction occurred when B_0 was near the *c* axis (Figure 1) for one phosphorus and near the *a* axis for the other. These axes are both perpendicular to the *b* axis, which, as we have seen, is close to the direction of minimum ^{95}Mo hyperfine interaction.

The matrices of $\mathbf{g}^2$ and $\mathbf{a}_{95}^2/MHz^2$ are presented in Table III, together with their principal values, the principal values of $\mathbf{g}$ and $\mathbf{a}_{95}/MHz$, and their respective direction cosines referred to the *abc* axis system.

Discussion

The average of the three principal values of the $\mathbf{g}$ matrix (1.9828) is in excellent agreement with the *g* factor of the spectrum obtained in *n*-pentane at 173 K, 1.9836, leaving no room for doubt that the carriers of the two spectra are the same molecule. Within experimental error, the $\mathbf{g}$ and $\mathbf{a}_{95}$ matrices are uniaxial and their unique directions are parallel to the unit vector (−0.2194, 0.9756, 0.0000) in the *abc* basis. This direction is clearly an important direction in the molecule, being associated with minimum ^{95}Mo hyperfine interaction and minimum *g* shift from that of a free spin, 2.0023. From Table I and the crystal symmetry, it may be calculated that one Mo–C(0) vector (where C(0) is a point at the center of the Cp ring) in orthorhombic crystals of $Cp^*MoCl(PMe_3)_2(N_2)$ is (−0.1953, 0.9723, 0.1285). The angle between these two vectors is 7.5°, a correlation that enables us to identify this direction with *z*, the 2-fold axis of the $Cp^*MoCl_2(PMe_3)_2$ molecule. If the apparently zero *bc* and *ac* off-diagonal elements of the ^{95}Mo hyperfine matrix (Figure 2b) are indeed zero (the data are rather sparse in *bc*, for reasons mentioned earlier), it would appear that the molecular 2-fold axis of $Cp^*MoCl_2(PMe_3)_2$ lies in the *ab* plane 12.7° from *b* (Figure 3), whereas in the host matrix the Mo–C(0) vector is 7.4° out of the *ab* plane. Normally, if the tensor axes lie skew in the crystal-axis system, a four-site spectrum[7] is observed for an arbitrary magnetic field direction, which coalesces to two-site spectra within crystal planes and to single-site spectra along the crystal axes. In the present instance, the combination of a large natural line width, the proximity of the tensor principal directions to crystal axes, and the complexity of the spectrum made the observation of individual-site spectra very difficult. Site-splitting was detected in the *ab* plane only (Figure 2, Table III), and even there only one of the sites gave a measurable spectrum. The apparent departure of the radical 2-fold axis by some 7° from the expected skew direction within the host crystal must, therefore, be accepted with caution.

It would appear at first glance that the Cp* ligand determines the remaining principal directions of $\mathbf{g}^2$ and $\mathbf{a}_{95}^2$. Thus, C1–C5 is the vector (0.9784, 0.2040, 0.0343), a direction only 2.1° from that of minimum *g* principal value and intermediate Mo hyperfine value. It is of course tempting to deduce from this correlation that certain symmetry elements of the Cp* ring determine the directions of $g_{xx,yy}$ and $a_{xx,yy}$. However, the near axiality of both

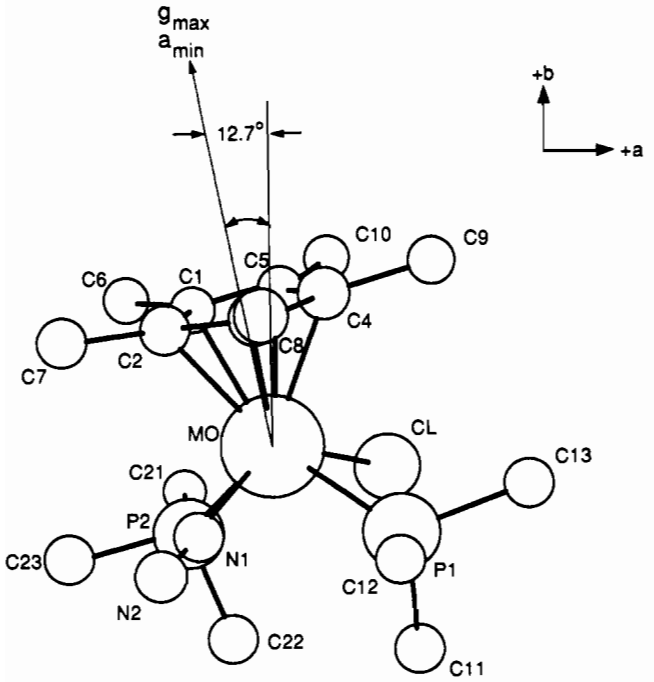

Figure 3. Projection of the crystallographic structure of $Cp^*MoCl(N_2)(PMe_3)_2$ along c, showing the directions of the unique principal values of **g** and $\mathbf{a}_{95}$.

matrices contributes to great uncertainty in the derived eigenvectors in the plane perpendicular to z and renders such correlations meaningless.

With z defined as the line through the molybdenum atom and the center of the Cp* ring, does the experimental evidence favor Mo $4d_{z^2}$ or Mo $4d_{xy}$ for the semioccupied orbital? The most unequivocal answer to this question is to be obtained from the nature of the ^{95}Mo hyperfine matrix. It has axial symmetry, as we have seen, with principal values that can be labeled $a_\parallel$ and $a_\perp$. The overall hyperfine interaction is the sum of two components, an anisotropic contribution A_{iso} and an isotropic contribution P. P is a number that is proportional to $\langle r^{-3}\rangle$ for the unpaired electron (r = instantaneous electron–nucleus distance) and to the magnetic moment of the nucleus. Since ^{95}Mo has a negative magnetic moment, P is a negative number. If the unpaired spin population is in Mo $4d_{z^2}$, a positive A_{iso} will result from spin polarization of the inner Mo s orbitals and the consequent negative Mo ns spin population and negative magnetic moment of ^{95}Mo.

A d_{z^2} semioccupied orbital will therefore have hyperfine interactions of the following form:[8]

$$a_\parallel = A_{iso} + (4/7)P \qquad a_\perp = A_{iso} - (2/7)P$$

If, on the other hand, the unpaired spin population is in Mo $4d_{xy}$

$$a_\parallel = A_{iso} - (4/7)P \qquad a_\perp = A_{iso} + (2/7)P$$

Since P is negative, spin population in Mo $4d_{z^2}$ will result in $a_\parallel \ll a_\perp$ whereas $4d_{xy}$ will give $a_\parallel \gg a_\perp$. In the present instance, the choice clearly favors $4d_{z^2}$, and so

$$a_\parallel - a_\perp = (6/7)P = \pm 10 - 137.5 = -127.5 \text{ or } -147.5 \text{MHz}$$

An estimate of P can thus be generated, namely $P = -149$ or -172 MHz. The former value is in excellent agreement with a value calculated from $\langle r^{-3}\rangle$ for a 4d Mo Hartree–Fock–Slater atomic orbital (−150.7 MHz)[8] and indicates that the unpaired electron is essentially confined to Mo $4d_{z^2}$.

The ordering of the Mo 5d atomic orbitals in $Cp^*MoCl_2(PMe_3)_2$ will now be considered, with a view of rationalizing its observed **g** matrix. Formally, the 3+ charge on the metal atom is compensated for by the cyclopentadienyl and chlorine ligands, each of which carries a formal negative charge. According to Hoffmann and co-workers,[3] in a square-pyramidal tetracarbonyl the five Mo d orbitals will have the following order (increasing energy): xy, z^2, (xz, yz), $x^2 - y^2$. The (xz, yz) electrons interact strongly with electrons on the negatively charged Cp* and Cl ligands, being further destabilized (raised). The electronic configuration is therefore $(xy)^2,(z^2)^1$, $^2A_1$ in C_{2v} symmetry. Spin–orbit interactions between the ground state and excited states associated with unpaired spin in the xz ($^2B_1$) and yz ($^2B_2$) orbitals are responsible for the negative g shift when B_0 is perpendicular to the z axis. A positive g shift when B_0 is placed along z (due to spin–orbit interaction with the $(xy)^1,(z^2)^2$ configuration) is possible in principle in C_{2v} symmetry, but not in C_{4v} symmetry. The absence of such a g shift is due to the fact that the orbital angular momentum operator l_z operating on d_{z^2} does not generate d_{xy}.

Poli and co-workers[4] have recently carried out Fenske–Hall type MO calculations on the model compound $CpMoCl_2(PH_3)_2$. For the calculations done without d orbitals on P, the major contribution to their semioccupied orbital (labeled 19a′) is Mo $4d_{z^2}$ (78%), but with small contributions also from each P 3p (0.66%) and P 3s (0.09%). As discussed above, the prediction of a dominant Mo $4d_{z^2}$ contribution to the semioccupied orbital is entirely consistent with the experimental facts. The computed phosphorus unpaired spin densities, however, appear to be too small. With estimates of $\langle r^{-3}\rangle$ for P 3p and of $\Psi^2(0)$ for P 3s of 4.242 and 7.252 au, respectively,[8] these figures lead to a predicted ^{31}P hyperfine interaction having principal values of approximately 17, 10, and 10 MHz. Spin-polarization effects could perhaps account for the disparity in experimental and theoretical isotropic ^{31}P hyperfine couplings. The anisotropy in the coupling was unfortunately not established quantitatively but did appear to be much larger than suggested by the Fenske–Hall calculations. Unfilled orbitals are at least 29 000 cm^{-1} higher than 19a′. If λ is the spin–orbit interaction for Mo^{3+} (ca. 817 cm^{-1}),[9] $\Delta g_\perp$ should be of the order of $-2\lambda(0.61)/29000$, or −0.034 (assuming 78% spin population in the interacting orbitals of the ground and excited states). This value is in excellent agreement with the observed value of −0.029.

Acknowledgment. R.T.B. wishes to thank T. J. Onley for fine technical assistance, P. J. Krusic and J. C. Calabrese for valuable discussions, and R. Poli for communication of results prior to publication.

Supplementary Material Available: Tables of calculated hydrogen atom positions and anisotropic thermal parameters (2 pages); complete listings of observed and calculated structure factors (13 pages). Ordering information is given on any current masthead page.

(8) Morton, J. R.; Preston, K. F. *J. Magn. Reson.* **1978**, *30*, 577.

(9) Goodman, B. A.; Raynor, J. B. *Adv. Inorg. Chem. Radiochem.* **1970**, *13*, 135.